MICROCOPY RESOLUTION TEST CHART
NATIONAL BUREAU OF STANDARDS – 1963 – A

ARO 19511.3-MS

②

TEMPERATURE COMPENSATION IN THE '2:17' TYPE MAGNETS

FINAL REPORT

K. S. V. L. Narasimhan, F. E. Camp,
Bao-Min Ma, C. J. Willman

MARCH 1986

DTIC
ELECTE
JUN 2 6 1986
S
D
D

U. S. ARMY RESEARCH OFFICE

CRUCIBLE MATERIALS CORPORATION
CRUCIBLE RESEARCH CENTER
PITTSBURGH, PA.

86

THE VIEW, OPINIONS, AND/OR FINDINGS CONTAINED IN THIS REPORT ARE THOSE OF THE
AUTHOR(S) AND SHOULD NOT BE CONSTRUED AS AN OFFICIAL DEPARTMENT OF THE ARMY
POSITION, POLICY, OR DECISION, UNLESS SO DESIGNATED BY OTHER DOCUMENTATION.

| REPORT DOCUMENTATION PAGE | | READ INSTRUCTIONS BEFORE COMPLETING FORM |
|---|---|---|
| **1. REPORT NUMBER** $ARO\ 19511.3-MS$ | **2. GOVT ACCESSION NO.** N/A | **3. RECIPIENT'S CATALOG NUMBER** N/A |
| **4. TITLE *(and Subtitle)*** Temperature Compensation in the '2:17' Type Magnets | | **5. TYPE OF REPORT & PERIOD COVERED** Final Report Jan. 1983 - Dec. 1985 |
| | | **6. PERFORMING ORG. REPORT NUMBER** |
| **7. AUTHOR(s)** K. S. V. L. Narasimhan, F. E. Camp, Bao-Min Ma, C. J. Willman | | **8. CONTRACT OR GRANT NUMBER(s)** DAAG29-83-C-0007 |
| **9. PERFORMING ORGANIZATION NAME AND ADDRESS** Crucible Materials Corporation Crucible Research Center P. O. Box 88, Pittsburgh, Pa. 15230 | | **10. PROGRAM ELEMENT, PROJECT, TASK AREA & WORK UNIT NUMBERS** |
| **11. CONTROLLING OFFICE NAME AND ADDRESS** U. S. Army Research Office Post Office Box 12211 Research Triangle Park, NC 27709 | | **12. REPORT DATE** March 1986 |
| | | **13. NUMBER OF PAGES** 17 |
| **14. MONITORING AGENCY NAME & ADDRESS*(If different from Controlling Office)*** | | **15. SECURITY CLASS. *(of this report)*** Unclassified |
| | | **15a. DECLASSIFICATION/DOWNGRADING SCHEDULE** |

**16. DISTRIBUTION STATEMENT *(of this Report)***

Approved for public release; distribution unlimited.

**17. DISTRIBUTION STATEMENT *(of the abstract entered in Block 20, if different from Report)***

NA

**18. SUPPLEMENTARY NOTES**

The view, opinions, and/or findings contained in this report are those of the author(s) and should not be construed as an official Department of the Army position, policy, or decision, unless so designated by other documentation.

**19. KEY WORDS *(Continue on reverse side if necessary and identify by block number)***

Magnets, Travelling Wave Tubes, Temperature Compensation, Sm-Co, Pr-Co, Nd-Co, NdFeB.

**20. ABSTRACT *(Continue on reverse side if necessary and identify by block number)***

Development of temperature compensated magnets was undertaken in both '2:17' and NdFeB type of alloys. A number of alloys have been identified that can produce energy product in excess of 40 MGOe in the uncompensated material. Computer programs were developed for identifying key compositions that were then processed successfully into temperature compensated magnets. Current materials can produce temperature compensated magnets with an energy product not exceeding 22 MGOe. Further work is necessary to develop temperature compensated magnets with an energy product exceeding 30 MGOe.

**DD** FORM 1473 JAN 73   EDITION OF 1 NOV 65 IS OBSOLETE

Temperature Compensation in the '2:17' Type Magnets

Pr and Nd Substituted '2:17' Magnets for Elevated
Temperature Application

The program was conducted in three phases. Phase I dealt with identifying composition ranges between $RCo_5$-$R_2Co_{17}$ that can produce maximum induction. Anisotropy field and saturation magnetization were measured on a series of Sm, Pr, and Nd alloys. The results indicate that Pr, Nd or a combination of both can be effectively utilized for increasing the saturation induction and yet maintain reasonable values of anisotropy field. Energy products greater than 40 MGOe are possible.

Phase II addressed the issue of temperature compensation in the '2:17' type of magnets to permit the utilization of these magnets in travelling wave tubes operating at 200-250°C. A computer assisted composition selection procedure was adopted that allowed pinpointing compositions that will yield best temperature compensation. Magnets fabricated from the identified compositions produced temperature coefficient that satisfied the program goals (+0.0008% per °C over a temperature range of -50 to room temperature and -0.007% per °C over room temperature to 250°C).

Phase III dealt with developing temperature compensation in the NdFeB type of alloys. Nearly 3000 compositions were generated through the computer. Combinations of light rare earth with heavy, heavy rare earth with heavy and two heavy rare earth with light rare earth were examined. Two compositions were chosen and processed into magnets.

Listed below are their composition, magnetic properties, and temperature coefficients.

Magnet #1: $(Nd_{0.24}Ho_{0.70}Er_{0.06})_{15}Fe_{79}B_6$, ATC-112 + 24% Alloy #6

$B_r$ = 7,900 Gauss
$H_c$ = 7,700 Oe
$H_{ci}$ = 14,400 Oe
$BH_{max}$ = 15.2 MGOe
$H_k$ = 13,000 Oe
Density = 7.8 gm/cc

| Temperature Range (°C) | Temperature Coefficient $\alpha$ (% per °C) |
|---|---|
| -50 to +150 | -0.0345 (-0.013 predicted) |
| -50 to +25 | +0.0081 |
| +25 to +100 | -0.0399 |

Magnet #2: $(Nd_{0.24}Ho_{0.64}Dy_{0.13})_{15}Fe_{79}B_6$, ATC-110 + 18% Alloy #4

$B_r$ = 7,700 Gauss
$H_c$ = 7,700 Oe
$H_{ci}$ = 20,600 Oe
$BH_{max}$ = 14.8 MGOe
$H_k$ = 18,300 Oe
Density = 7.98 gm/cc

| Temperature Range (°C) | Temperature Coefficient $\alpha$ (% per °C) |
|---|---|
| -50 to +150 | -0.0299 (-0.012 predicted) |
| -50 to +75 | -0.0033 |
| -25 to +75 | -0.0066 |
| -50 to 0 | +0.0152 |

A-1

## TEMPERATURE COMPENSATION IN THE '2:17' TYPE MAGNETS

F. E. Camp, K. S. V. L. Narasimhan, and J. C. Hurt

### ABSTRACT

Compensation for the temperature dependence of magnetic flux has been investigated in the '2:17' type permanent magnet alloys. A computer assisted composition selection procedure was adapted and one of the identified compositions, $Sm_{1.18}Dy_{.81}Gd_{.01}Co_{9.76}Fe_{4.19}Cu_{.83}Zr_{.34}$, was processed into magnets. The measured temperature coefficients correlated satisfactorily with the prediction. Dysprosium was found to be a better substituent for Sm than either Gd or Er in providing temperature coefficient of linearity.

### INTRODUCTION

Temperature compensated magnets have found application in devices such as gyros, accelerometers, and to a certain extent, in travelling wave tubes. Samarium cobalt magnets have been successfully temperature compensated by alloying with heavy rare earths[1-4]. For a fully compensated $SmCo_5$ magnet, the maximum energy product attainable is 7.0 MGOe[5]. Further miniaturization of devices is possible only if the $BH_{max}$ is increased further to possibly 16-20 MGOe. We have investigated rare earth-cobalt '2:17' type of alloys to improve the $BH_{max}$ of a fully compensated magnet.

Temperature compensation in '2:17' type alloys has been investigated by various authors[6,7]. However, a generalized approach for identifying the alloys that can provide the needed temperature coefficient has not been made. Such an approach is necessary to permit alloy development suited to the need of a particular device since the flux in the gap is dependent not only on the characteristics of the magnet but also on the temperature variation of the device gap. This publication presents an analytical approach to composition selection and the results on an alloy from this selection.

### EXPERIMENTAL

The molar composition of the base alloy was $Sm_2Co_{9.76}Fe_{4.19}Cu_{.83}Zr_{.34}(Sm_2TM_{15})$. This and four heavy rare earth analogs, $SmDyTM_{15}$, $SmErTM_{15}$, $SmGdTM_{15}$, and $SmHoTM_{15}$ were each induction melted under argon gas and cast into split copper molds. The ingots were crushed to 75μm powder and thermomagnetic measurements made over the temperature range of -60°C to 220°C. The Faraday technique was used with an applied field of 5 kilo-oersteds.

The composition that was predicted to have the smallest temperature coefficients was $Sm_{1.18}Dy_{.81}Gd_{.01}TM_{15}$. It was induction melted by the above procedure and pulverized to -60 mesh powder. Jet milling with argon gas produced an average particle size of ~5 microns. The base alloy, $Sm_2TM_{15}$, was also jet milled to ~5 microns. Magnets (1cm diameter x 7cm long) were pressed, sintered between 1150-1200°C for 1 hour, solutionized for 5 hours between 1120-1160°C, then quenched. They were then further heat treated at 800-850°C and slowly cooled to 400°C then naturally cooled to room temperature.

Camp and Narasimhan are with Colt Industries, Crucible Research Center, Pittsburgh, PA 15230, and Hurt is with the Army Research Office, Research Triangle Park, NC 27709.

After hysteresis loops were determined for centerless ground and cut samples, temperature coefficients of magnetization were measured with an oscillating sample magnetometer. The magnetized sample (0.75cm diameter x 3cm long) and the pick-up coil were positioned within a cooling/heating environmental chamber. When thermal equilibrium was reached, the sample was driven through the coil at a constant speed. The magnetic flux so generated was measured and integrated over the length with a 6.5 digit voltmeter input to a desk computer.

### RESULTS AND DISCUSSION

The thermomagnetic data determined by the Faraday technique are shown in Figure 1. The base alloy has a large negative temperature coefficient of magnetization over the entire temperature range, while the curves for the alloys containing Dy, Er, Gd, or Ho show less variation and have positive temperature coefficients in their cooler regions. This phenomenon, which is typical of heavy and light rare earth-transition metal (Fe, Co) alloys of the 1:5 and 2:17 stoichiometry, suggests a method of approaching temperature independence of magnetization with the judicious selection of heavy rare earth combinations and concentrations.

We have generated a number of theoretical magnetization curves from these experimental data. A simplifying assumption was made that, at a given temperature, magnetization is an additive property with the number of rare earth atoms. Implicit in this assumption is that crystal field effects are unchanged by the addition of heavy rare earths.

Incremental interpolations were calculated between the base alloy and each heavy rare earth analog. These interpolations resulted in families of curves or data arrays for each heavy rare earth. A large number of magnetization vs temperature curves were then computer generated from these data arrays. Various concentrations of either two, three, or all four heavy rare earths were considered.
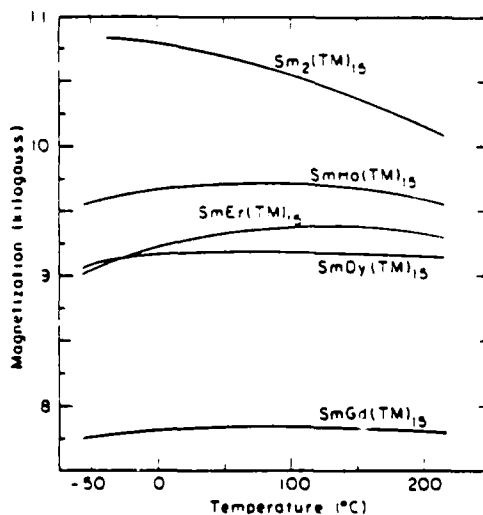


Figure 1. Magnetization vs temperature data measured for the Sm and heavy rare earth substituted for Sm alloys. $TM=Co_{9.76}Fe_{4.19}Cu_{.83}Zr_{.34}$.

Due to space limitations, we have selected certain families of curves for inclusion here on the basis of two criteria--those showing the greater linearity, and others displaying the effects of all the heavy rare earths considered. Figures 2, 3, 4 and 5 show the hypothetical curves for two heavy rare earth additives. The formulations predicting the lowest temperature coefficients are shown on these figures and are listed in Table I. The coefficients were calculated by the least squares method.
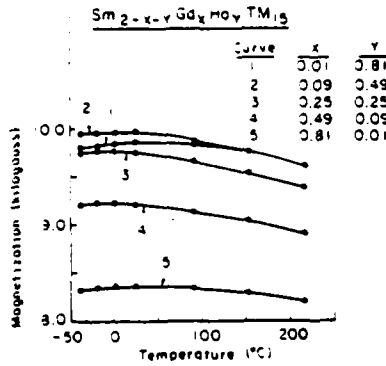


Figure 2. Computer generated curves for the Gd and Ho substituted alloys.
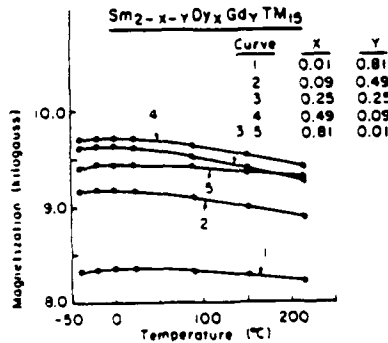


Figure 3. Computer generated curves for the Dy and Gd substituted alloys.
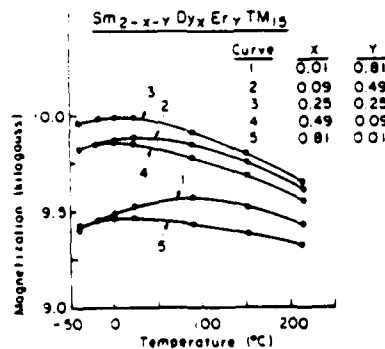


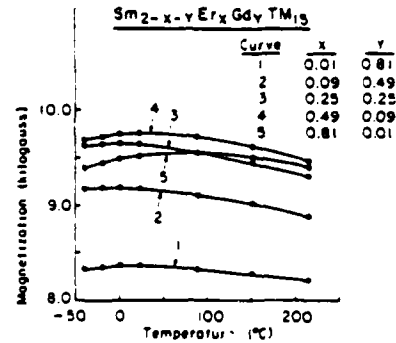Figure 4. Computer generated curves for the Dy and Er substituted alloys.



Figure 5. Computer generated curves for the Er and Gd substituted alloys.

Table I. Alloys with Predicted Low Temperature Coefficients of Magnetization

| | Temperature Coefficient, $\%°C^{-1}$ | |
|---|---|---|
| Alloy | −50 to 25°C | 25°C to 250°C |
| $Sm_{1.18}Dy_{.81}Gd_{.01}TM_{15}$ | +.00624 | −.00788 |
| $Sm_{1.18}Gd_{.81}Ho_{.01}TM_{15}$ | +.00713 | −.00793 |
| $Sm_{1.42}Er_{.09}Gd_{.49}TM_{15}$ | +.00298 | −.0164 |
| $Sm_{1.18}Gd_{.81}Dy_{.01}TM_{15}$ | +.00705 | −.00901 |
| $Sm_{1.18}Ho_{.81}Gd_{.01}TM_{15}$ | +.012 | −.0121 |

Figures 6 and 7 show typical curves for three heavy rare earth components, and Figure 8 contains some curves for all four heavy rare earths. There is less linearity exhibited in these multi-component predictions than was evident in the two component results.

The alloy predicted to have the lowest temperature coefficient, $Sm_{1.18}Dy_{.81}Gd_{.09}TM_{15}$, was prepared and fabricated into a magnet. The following magnetic properties were measured: $B_r$=8,900 Gauss, $H_{ci}$=7,750 Oersted, $H_c$=6,300 Oersted, and $BH_{max}$=16.5 MGOe. The results of temperature coefficient measurements are shown in Figure 9 along with the predicted curve for this alloy. Although the experimental curve lies below the predicted curve (absolute magnetization values smaller by 5%), there is good agreement between the shapes of the curves and their respective slopes. The low temperature coefficients are +.0008$\%°C^{-1}$(experimental) versus +.00624$\%°C^{-1}$(predicted). The other set of coefficients is −.00774$\%°C^{-1}$(experimental) and −.00788$\%°C^{-1}$(predicted). This is indicative of the validity of this procedure to predict the general shape of magnetization versus temperature curves for various alloys incorporating heavy rare earths for temperature compensation.

Previous work has shown the temperature compensation benefits of Gd[8] and Er[7], with which we concur. The former has the disadvantage of lowering magnetization values more so than others. We have shown that Dy is also an excellent candidate. It will provide linearity over a broader temperature range than Er does. This is graphically displayed by comparing curves 1 and 5 in Figure 4, where the higher Dy content (Curve 5) shows less variation over the −50°C to 222°C temperature range than the corresponding Er curve.

2

It is also displayed by noting the difference in curve shapes between Figures 6 and 7, where Dy and Er, respectively, are dominant in otherwise identical ternary heavy rare earth systems. Dy has an additional economic advantage as being the least expensive of the four heavy rare earths considered.
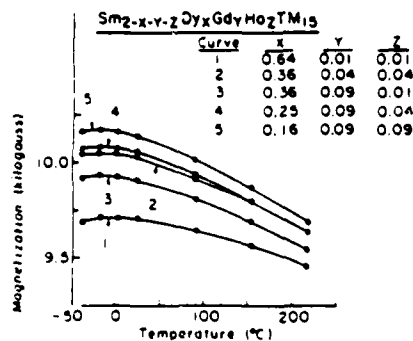
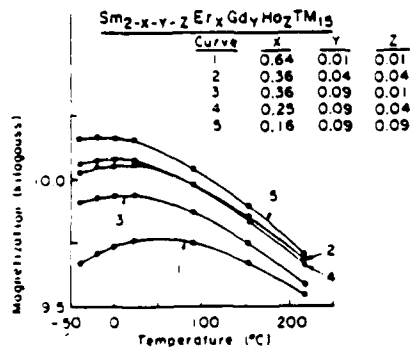Figure 6. Computer generated curves for three component rare earth alloys.

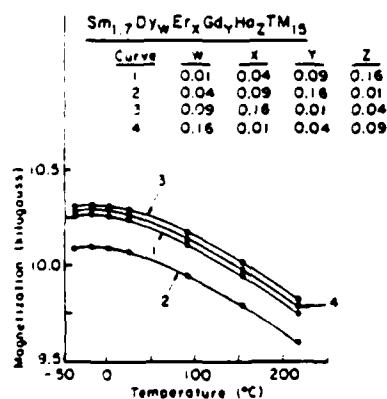Figure 7. Computer generated curves for three component rare earth alloys.

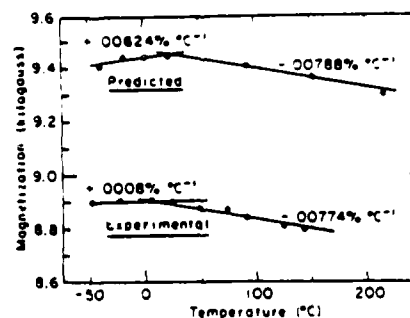Figure 8. Computer generated curves for four component rare earth alloys.

Figure 9. Experimental and predicted temperature dependence of magnetization data for $Sm_{1.18}$ $Dy_{.81}Gd_{.01}TM_{15}$ alloy. The numbers on the curves refer to the temperature coefficient of magnetization over the low ($-50^{\circ}$ to $0^{\circ}C$) and high temperatures ($0^{\circ}$ to $250^{\circ}C$).

## CONCLUSIONS

The proposed method of predicting the behavior of heavy rare earth additions to alloy systems may be used in place of the "trial and error" procedures. Dy additions result in improved temperature compensation over a broad temperature range. Gd is effective over the same range, but significantly lowers the magnetization. Erbium will give results similar to Dy, but over a smaller temperature range. Dy has the added advantage of being the least expensive.

## REFERENCES

1. M. G. Benz, R. P. Laforce and D. L. Martin, AIP Conf. Proc., No. 18, 1173 (1974).

2. F. G. Jones and M. Tokunaga, IEEE Trans. Magn., Vol. MAG-12, 968 (1976).

3. K. S. V. L. Narasimhan, M. G. H. Wells and D. V. Ratnam, J. App. Physics, 49, 2072, (1978).

4. K. S. V. L. Narasimhan, J. App. Physics, Vol. 52, No. 3, 2512 (1980).

5. K. S. V. L. Narasimhan, Fifth International Workshop on Rare Earth-Cobalt Permanent Magnets and Applications, Roanoke, Va., June 1981, University of Dayton, 629 (1981).

6. F. Rothwarf, H. A. Leupold, A. Tauber, J. T. Breslin, R. L. Bergner and J. J. Winter, The Rare Earths in Modern Science and Technology, Vol. 2, edited by G. J. McCarthy, J. J. Rhyne and H. B. Siber (Plenum, New York 1980).

7. H. F. Mildrum, J. B. Krupar and A. E. Ray, J. Less-Common Met. 93, 261 (1983).

8. R. L. Bergner, H. A. Leupold, J. T. Breslin, F. Rothwarf and A. Tauber, J. App. Physics, 50, 2349, (1979).

# Pr AND Nd SUBSTITUTED '2:17' MAGNETS
## FOR ELEVATED TEMPERATURE APPLICATION

C. J. Willman and K. S. V. L. Narasimhan

### ABSTRACT

Results of Pr, Nd and (PrNd) substitution in the
'2:17' type permanent magnet alloys are presented.
Microstructural studies, crystal structure, anisotropy
field ($H_A$), Curie temperature ($T_c$), and saturation
magnetization ($M_s$) were used as tools for the evalua-
tion of these alloys. Pr, Nd and (PrNd) increases $M_s$
without significantly affecting the $T_c$. $H_A$ decreases
when Sm is replaced by Pr, Nd or (PrNd). Several of
the alloys investigated show promise to be permanent
magnets.

### INTRODUCTION

'2:17' type of permanent magnets have been in
production for the last several years. The general
stoichiometry is about $RM_{7.5-7.7}$ where M is a combin-
ation of Fe, Co, Cu, $Zr^{1,2}$. The maximum energy
product attainable is 33 MGOe². Further increase in
the $BH_{max}$ is possible if the saturation magnetization
($M_s$) is increased by increasing the number of moment
carrying atoms, i.e., Fe and Co. Samarium has a very
small magnetic moment to contribute. Shimoda et al[3]
and Ray et al[4] have increased the M value from 7.4 to
8.35 by increasing the iron content and successfully
made magnets. The $M_s$ value reported was 11,500 -
11,800 Gauss. The maximum energy product attainable
is 33-35 MGOe assuming the anisotropy field is high
and $BH_{max}$ can be approximated to $B_r^2/4$. The increase
in iron content alone is not able to increase the
saturation magnetization past 12,000 Gauss. It is
possible to increase the induction by decreasing the
copper content since copper acts as a diluent for the
magnetic moment. However, copper is vital for the
generation of coercive force and hence cannot be
reduced significantly. We, therefore, added Pr and
Nd to increase the saturation induction and the
results of these investigations are presented in
this paper.

### EXPERIMENTAL PROCEDURE

The alloys were prepared by induction melting
the elements and casting the alloy into a copper
mold.

1. K-ray Data: X-ray diffraction data was obtained
   using a Norelco X-ray Generator (40kV, 12mA) in
   conjunction with a 114.7 Debye Scherrer camera.
   CrKα radiation was used on -100 mesh alloy pow-
   der. The resulting powder patterns were indexed.
   An iterative least squares technique was used to
   calculate the lattice parameters of each alloy.

2. Curie Temperature Evaluation: Homogenized alloy
   was crushed to -100 mesh and TMA (thermomagnetic
   analysis) was used to determine $T_c$ and other
   magnetic phases. A field of 1 kOe was used for
   this study.

3. Saturation Magnetization: Homogenized alloy was
   crushed and ground to -400 mesh in argon. Ali-
   quots of 50-80 mg were measured into the VSM
   (vibrating sample magnetometer) holder. The VSM
   was calibrated with a Ni standard using $\sigma_{Ni}$ =
   54.40 emu/g at 295K. Honda plots were extrap-
   olated to obtain σ saturation.

Willman and Narasimhan are with Colt Industries,
Crucible Research Center, Pittsburgh, PA 15230.

4. Anisotropy Field: Alloy was crushed to -325
   mesh. The powder was then dispersed in paraffin
   wax and aligned in a 25 kOe field and allowed to
   harden in the presence of a field. The field
   required to saturate in the direction parallel
   and perpendicular to the easy direction were
   evaluated. $H_A$ was determined as the field
   required to saturate the material in the
   perpendicular direction.

### DISCUSSION

The X-ray diffraction patterns of the alloys
studied could be indexed to a $Th_2Ni_{17}$ (hexagonal)
type structure. This structure is characteristic
of high-temperature, disordered $Sm_2Co_{17}$[5]. The as-
cast alloys were 2-phase. With increased Fe sub-
stitution for Co and with rare earth substitutions
for Sm, more complex microstructures were observed.
Homogenization of the as-cast structure was
possible between 1165-1185°C for most alloys (see
Figures 1 through 3). Those alloys having complex
microstructures were more difficult to homogenize.



| Figure 1a 125X | Figure 1b 125X |
|---|---|
| *x=0, v=0.2 | *x=0, v=0.2 |
| Prior to Heat Treatment | After Heat Treatment |



| Figure 2a 125X | Figure 2b 125X |
|---|---|
| *RE=Nd, x=0.1, v=0.2 | *RE=Nd, x=0.1, v=0.2 |
| Prior to Heat Treatment | After Heat Treatment |



| Figure 3a 125X | Figure 3b 125X |
|---|---|
| *RE=Nd, x=0.3, v=0.4 | *RE=Nd, x=0.3, v=0.4 |
| Prior to Heat Treatment | After Heat Treatment |
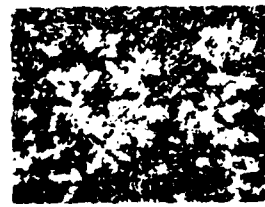
$*Sm_{1-x} RE_x Co_{.90-w} Fe_w Cu_{.08} Zr_{.02}$ v=.55

Most secondary phases were able to be solutionized
with the exception of a white phase. This phase
was determined to be an Fe-Co rich phase. The
presence of this phase was particularly prominent
in those alloys (as-cast condition) having the
largest substitutions of Fe for Co (v=0.3, 0.4).

Figures 4 and 5 illustrate the magnetization vs
temperature plots obtained for these alloys. As
expected, Fe substitution for Co was found to decrease
the Curie temperature. Pr, Nd, 50%Pr-50%Nd substitu-
tion for Sm did not affect the Curie temperature sig-
nificantly.

The saturation magnetization of these alloys
increases with increasing Fe, Pr, Nd, or Pr/Nd sub-
stitutions. Some of the alloy samples were exception-
ally difficult to saturate and consequently $M_s$ was more
difficult to measure.



Figure 5.  Temperature dependence of magnetization at
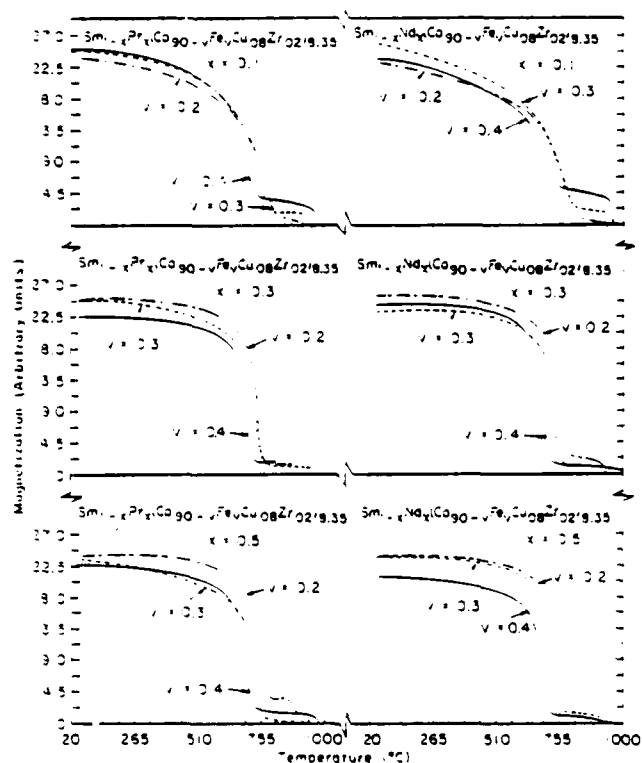an applied field of 1 kOe.



Figure 4.  Temperature dependence of magnetization at
an applied field of 1 kOe.

Table I illustrates the magnetization observed at
an applied field of 18 kG, and the value of the mag-
netization extrapolated to infinite field. Calculation
of the theoretical $3H_{max}$ ($B_s^2/4$) is also included in
Table I.

The substitution of Pr, Nd, Pr/Nd for Sm in most
cases decreased the anisotropy field, $H_A$. Fe substitu-
tion for Co usually decreased the anisotropy field.
The effect of these substitutions is illustrated in
Figures 6 and 7. Nd and Pr in the '2:17' alloys prefer
a basal plane[6] and substitution of these elements re-
duces the overall preference of the rare earth sub-
lattice to the magnetically easy C-direction, hence a
decreased anisotropy field. The preference of iron
sublattice in the '2:17' alloy is in the basal phase
and the effect of iron substitution is also to
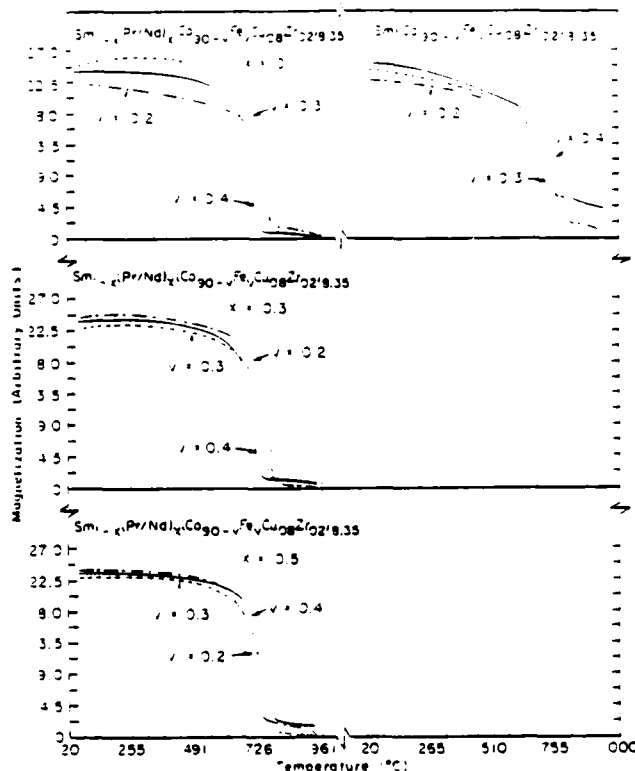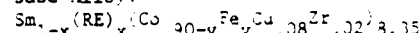decrease the anisotropy field.

Table I.  Base Alloy:
$$Sm_{1-x}(RE)_x(Co_{.90-v}Fe_vCu_{.08}Zr_{.02})_{8.35}$$

The results indicate that Pr, Nd, or a combination of both can be effectively utilized for increasing the saturation induction and yet maintain reasonable values of anisotropy field. These alloys could be used for the fabrication of magnets. In an alloy containing x=0.3, a combination of Pr and Nd is more effective in maintaining the anisotropy field than either Nd or Pr alone. This effect may be related to subtle crystal field effects that changes the stabilization energy.

$Sm_{1-x}(Pr_x Co_{30-y}Fe_y Cu_{0.8}Zr_{0.2})_{7.15}$

|  | y=0.2 | y=0.3 | y=0.4 |
|---|---|---|---|
| x=0.1 | 39 | 57 | 58 |
| x=0.2 | 38 | 55 | 5 |
| x=0.3 | 56 | 55 | 55 |
| x=0.5 | 49 | 39 | 25 |

$Sm_{1-x}(Nd_x Co_{30-y}Fe_y Cu_{0.8}Zr_{0.2})_{7.15}$

|  | y=0.2 | y=0.3 | y=0.4 |
|---|---|---|---|
| x=0.1 | 39 | 57 | 58 |
| x=0.2 | 52 | 58 | 60 |
| x=0.3 | 54 | 33 | 37 |
| x=0.5 | 52 | 22 | 31 |

$Sm_{1-x}(Pr/Nd)_x Co_{30-y}Fe_y Cu_{0.8}Zr_{0.2})_{7.15}$

|  | y=0.2 | y=0.3 | y=0.4 |
|---|---|---|---|
| x=0.1 | 39 | 57 | 58 |
| x=0.2 | 54 | 57 | 35 |
| x=0.3 | 60 | 55 | 24 |
| x=0.5 | 39 | 29 | 24 |

Figure 6. Anisotropy field matrix for alloys studied.
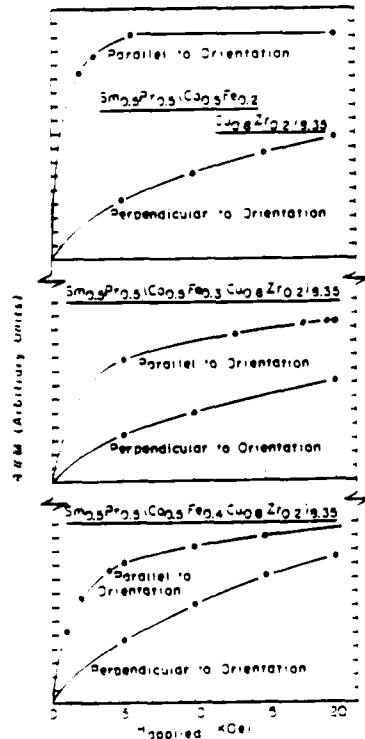


Figure 7. Typical magnetization vs $H_A$ in easy and hard directions for one set of alloys.

## CONCLUSION

The effect of Pr, Nd or a combination of Pr and Nd is to increase the saturation magnetization without adversely effecting the anisotropy field. A few of the compositions show promise for utilization as permanent magnets. The potential energy product of several of the alloys exceed 40 MGOe.

## Acknowledgments

## REFERENCES

1. T. Ojima, S. Tomizawa, T. Yoneyama and T. Hori. IEEE Trans. Mag., MAG-13, p. 1317 (1977).

2. R. K. Mishra, G. Thomas, T. Yoneyama, A. Fukuno and T. Ojima, J. Applied Physics, 52, p. 2517 (1981).

3. T. Shimoda, I. Okonogi, K. Kasai and K. Teraishi, IEEE Trans. Mag., MAG-16, p. 991 (1980).

4. A. E. Ray, H. F. Mildrum and J. B. Krupar, IEEE Trans. Magnetics, MAG-19, p. 2044 (1983).

5. (a) Y. Khan, Acta Cryst. 1329, p. 2503 (1973).
   (b) W. Ostertag and K. Strnat, Acta Cryst. 21, p. 560 (1966).

6. W. E. Wallace and K. S. V. L. Narasimhan, "Science and Technology of Rare Earths," p. 393-413, Academic Press, 1980; edited by E. C. Subbarao and W. E. Wallace.

7. K. S. V. L. Narasimhan, W. E. Wallace, R. D. Hutchens and J. E. Greedan, AIP Conf. Proc. 18, p. 1212 (1973).

# NdFeB MAGNETS WITH ZERO TEMPERATURE COEFFICIENT OF INDUCTION

Bao-Min Ma, K. S. V. L. Narasimhan*,
and J. C. Hurt**

*Crucible Materials Corporation
Crucible Research Center
P. O. Box 88, Pittsburgh, Pa.  15230

**U. S. Army Research Office
P. O. Box 12211
Research Triangle Park, N. C.  27709

## ABSTRACT

Temperature compensation for the induction of NdFeB type magnets has been investigated.  A computer assisted alloy selection method was adopted to identify composition of zero temperature coefficient of induction over -50 to 200°C.  Selected alloys were processed into magnet by the conventional powder metallurgy method.  The experimental temperature coefficient on the sintered magnet correlated with the prediction satisfactory.  Holmium is an essential ingredient required for temperature compensation of NdFeB magnets.  A magnet, $(Nd_{0.23}Ho_{0.64}Dy_{0.13})_{15}Fe_{79}B_6$ with $B_r$ of 7,700 Gauss, $H_c$ of 7,700 Oe, $H_{ci}$ of 20,600 Oe, $BH_{max}$ of 14.8 MGOe and temperature coefficient of -0.029% per °C over -50 to +150 was obtained.

## INTRODUCTION

Neodymoum-iron-boron magnets have high energy product [1-3].  However, the temperature dependence of magnetic induction is about -0.08% to -0.12% per °C over -50 to 150°C.  We have investigated heavy rare earth alloying to improve the temperature dependence.  A computer assisted composition selection procedure developed for $SmCo_5$ and the 2:17 [4-7] alloys has been extended to NdFeB alloys.

In excess of 3000 alloy compositions were generated from the magnetization data of $Nd_2Fe_{14}B$ and $HRE_2Fe_{14}B$ alloys.  The magnetization of $(NdHRE)_2Fe_{14}B$ was computed by adding the Nd and HRE moment linearly. The details are presented in this publication.

## EXPERIMENTAL

A data base of the temperature dependence magnetization and anisotropy field of $Nd_2Fe_{14}B$ as well as $HRE_2Fe_{14}B_8$ (where HRE = Ho, Dy, Er, Tm and Tb) were constructed over -50°C to +250°C at 25°C intervals.

The substitution of heavy rare earth was assumed to replace the Nd sites. The magnetization of the combination of $NdHRE_2Fe_{14}B$ was calculated by adding the Nd and heavy rare earth moment linearly. The temperature coefficient $\alpha$ is defined as:

$$\alpha \ (\% \ per \ {}^{\circ}C) = 100\% * [M(T_2)-M(T_1)]/[M(T_1)*(T_2-T_1)]$$

and calculated by a least square linear fitting. A Hewlett-Packard 85 computer with memory space of 32K was utilized to conduct these calculations.

Two criteria were set for the composition selection: (1) the selected composition must have a saturation magnetization greater than 7,500 Gauss at $25^{\circ}C$, and (2) the temperature coefficient of the induction must be less than $-0.01\%$ per $^{\circ}C$ over $-50$ to $+200^{\circ}C$. The replacement of Nd with each individual heavy rare earth were scanned from 0 to 100% at 2% increments. Both the temperature dependence magnetization curve and temperature coefficient $\alpha$ were examined simultaneously. Neodymium mixed with two or three heavy rare earths were also examined at 2% increments respectively.

Selected alloy compositions were prepared by vacuum induction melting and cast into a copper mold. Ingots were processed into magnets by the traditional powder metallurgy method utilizing a process similar to that used for $SmCo_5$.

The temperature coefficient of induction, $\alpha$, of the sintered magnets with length to diameter ratio (L/D) of 1.0-1.2 were measured by the open circuit technique (OCT) [8] from $-50$ to $+150^{\circ}C$ at $25^{\circ}C$ intervals. The demagnetization curves of the sintered magnets were also measured by closed circuit technique (CCT) for the same temperature range.

The Curie temperature of the cast alloy or sintered magnet were measured by thermomagnetic analysis (TMA) under an applied field of 4 kOe. Samples were crushed to $-400$ mesh powder then sealed under inert atmosphere into a Vycor capsule for measurement.

## RESULTS AND DISCUSSION

Two of the $R_2Fe_{14}B$ alloys, $Dy_2Fe_{14}B$ and $Tb_2Fe_{14}B$, have temperature coefficient $\alpha$ less than $-0.01$ per $^{\circ}C$ as shown in Table I.

Table I. The Saturation Magnetization $M_s$ at 25°C and Temperature Coefficient of Heavy Rare Earth $HRE_2Fe_{14}B$ Alloys

| $R_2Fe_{14}B$ R= | $M_s$ (Gauss) | Temperature Coefficient % per °C(−50 to +200) |
|---|---|---|
| Ho | 7,060 | +0.016 |
| Tb | 5,970 | −0.007 |
| Dy | 6,160 | +0.007 |
| Gd | 7,450 | −0.053 |
| Er | 7,890 | −0.042 |
| Tm | 9,810 | −0.078 |

Owing to the higher magnetic moment of $Nd_2Fe_{14}B$, the combination of Nd with one of the heavy rare earth results in an increased magnetization. The slope of the overall curves can also be adjusted by varying the relative amount of Nd–HRE combination. Illustrated in Figure 1 are the temperature dependence magnetization curves of $(Nd_{1-x}Ho_x)_2Fe_{14}B$, where x = 0 to 1.0 in steps of 0.2.



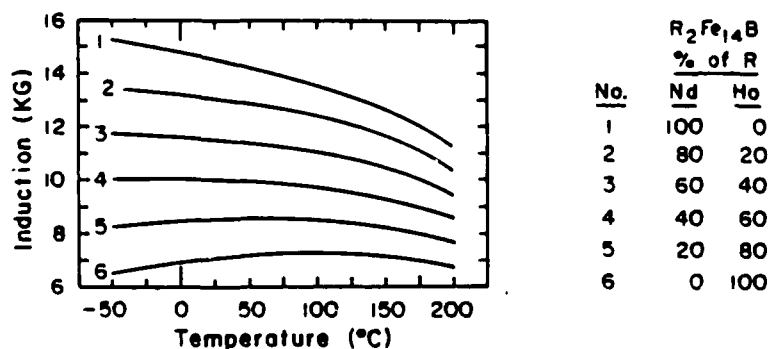| $R_2Fe_{14}B$ | | |
|---|---|---|
| | % of R | |
| No. | Nd | Ho |
| 1 | 100 | 0 |
| 2 | 80 | 20 |
| 3 | 60 | 40 |
| 4 | 40 | 60 |
| 5 | 20 | 80 |
| 6 | 0 | 100 |

Figure 1. Computer simulated temperature dependence magnetization curves of $(Nd_{1-x}Ho_x)_2Fe_{14}B$, where x = 0, .2, .4, .6, .8, and 1.0.

The combination of Nd with other single heavy rare earth were also examined for the entire composition range at 2% increments. Similarly, a combination of Nd with either two or three heavy rare earths were examined. Listed in Table II are the representative compositions of low temperature coefficient alloys with their saturation magnetization at 25°C.

Table II.  The Saturation Magnetization at 25°C and
the Temperature Coefficient of $R_2Fe_{14}B$
Type Magnet Generated by Computer Aid
Alloy Composition Selection Method

| % of Rare Earth in $R_2Fe_{14}B$ | | | | | | | Ms(25) | Temperature Coefficient (% per °C) | |
| Nd | Ho | Dy | Gd | Er | Tm | Tb | (Gauss) | -50 to 150 | -50 to 200 |
|---|---|---|---|---|---|---|---|---|---|
| 9 | 91 | | | | | | 7800 | +0.021 | -0.006 |
| 8 | 85 | | 7 | | | | 7700 | +0.018 | -0.008 |
| 5 | 85 | | | | 10 | | 7710 | +0.021 | -0.008 |
| 10 | 55 | 35 | | | | | 7400 | +0.015 | -0.009 |
| 8 | 85 | | | 7 | | | 7720 | +0.021 | -0.007 |
| 6 | 85 | | | | 9 | | 7780 | +0.020 | -0.010 |
| 10 | 86 | | | | | 4 | 7770 | +0.017 | -0.008 |
| 10 | 72 | 16 | 2 | | | | 7650 | +0.015 | -0.010 |
| 14 | 40 | 40 | 6 | | | | 7710 | -0.000 | -0.021 |
| 8 | | 38 | 52 | | | 2 | 7680 | +0.001 | -0.035 |
| 8 | 84 | | | | 6 | 2 | 7770 | +0.019 | -0.009 |

Figures 2 and 3 show the computer simulated curves
for various heavy rare earth containing $Nd_2Fe_{14}B$
alloys.  From these curves, selected alloy composi-
tions were processed into magnets.  The properties
of these low temperature coefficient magnets are
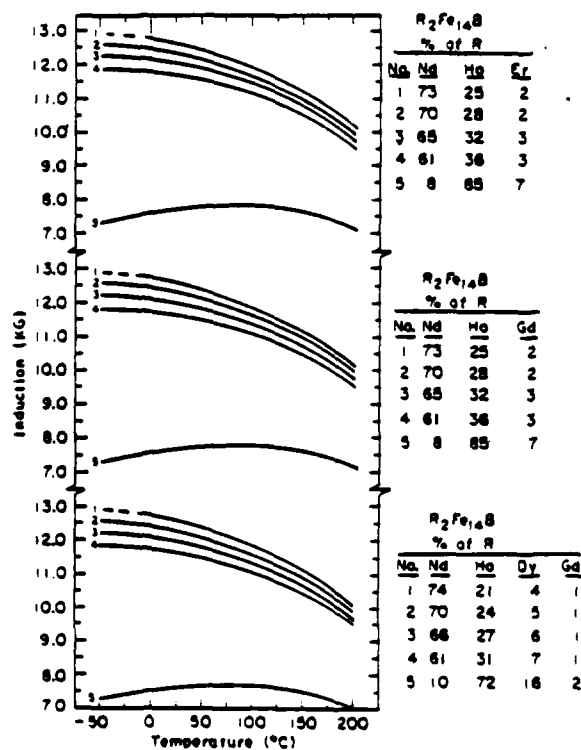listed in Table III.



Figure 2.  Computer simulated temperature dependence
magnetization curves of $(NdHoEr)_2Fe_{14}B$,
$(NdHoGd)_2Fe_{14}B$, and $(NdHoDyGd)_2Fe_{14}B$ on
the corresponding sintered magnets with
slightly higher Nd content.
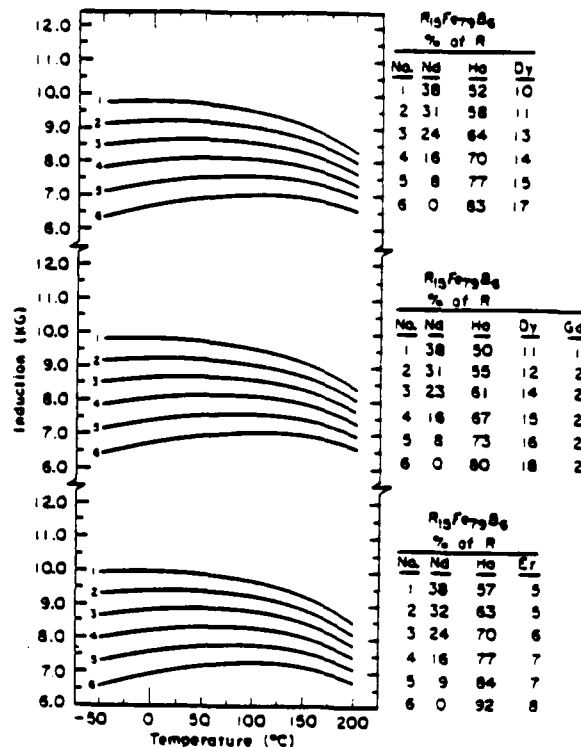
Figure 3. Computer simulated temperature dependence magnetization curves of $(NdHoDy)_2Fe_{14}B$, $(NdHoDyGd)_2Fe_{14}B$ and $(NdHoEr)_2Fe_{14}B$ of the corresponding low temperature coefficient sintered magnets.

Table III. Magnetic Properties of Temperature Compensated $R_2Fe_{14}B$ Type Magnet

| % of R in $R_2Fe_{14}B$ | | | | | | $B_R$ (Gauss) | $H_C$ (Oe) | $H_{CI}$ (Oe) | $BH_{MAX}$ (MGOe) | $H_K$ (Oe) | Density (gm/cc) |
|---|---|---|---|---|---|---|---|---|---|---|---|
| Ho | Dy | Er | Tm | Gd | | | | | | | |
| 65 | 35 | - | - | - | - | 9,800 | 9,400 | 16,450 | 22.8 | 14,400 | 7.35 |
| 60 | 36 | - | - | 4 | - | 8,800 | 7,700 | 11,950 | 16.8 | 6,400 | 7.06 |
| 61 | 36 | - | 3 | - | - | 8,900 | 8,800 | 14,900 | 20.3 | 10,500 | 7.24 |
| 32 | 63 | - | 5 | - | - | 7,900 | 7,700 | 14,400 | 15.2 | 13,000 | 7.80 |
| 65 | 32 | - | - | - | 3 | 8,900 | 7,750 | 10,850 | 17.6 | 8,700 | 7.11 |
| 61 | 31 | 7 | - | - | 1 | 9,350 | 9,000 | 20,470 | 20.3 | 19,850 | 7.44 |
| 24 | 64 | 12 | - | - | - | 7,700 | 7,700 | 20,600 | 14.8 | 18,300 | 7.98 |

Two magnets with the nominal composition of $(Nd_{0.24}Ho_{0.70}Er_{0.06})_{15}Fe_{79}B_6$, magnet A, and $(Nd_{0.23}Ho_{0.64}Dy_{0.13})_{15}Fe_{79}B_6$, magnet B, were selected for (1) the closed circuit temperature dependence demagnetization curve measurement and (2) the open circuit temperature dependence of induction measurements. Figures 4 and 5 are the temperature dependence demagnetization curves of these two magnets. The temperature dependence magnetic properties of these two magnets are summarized in Figure 6a and 6b respectively. In figures 7 and 8, the temperature dependence magnetization curves of magnet A and B are normalized to their values of $-50^{\circ}C$. Shapes of the

Shapes of the computer generated curves and the
experimental curves favorably compare. The
temperature coefficients are tabulated in
Table IV. The other two magnets with higher Nd
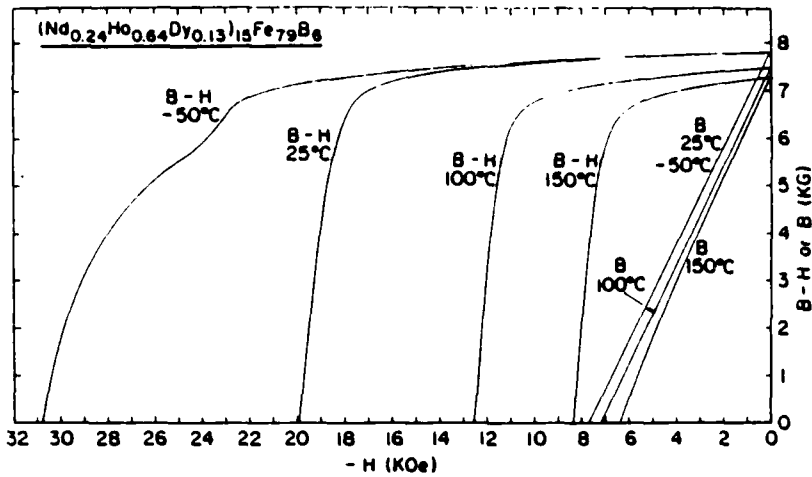contents are also listed for comparison.



Figure 4. The temperature dependence demagnetization
curves of $(Nd_{0.23}Ho_{0.70}Dy_{0.13})_{15}Fe_{79}B_6$.
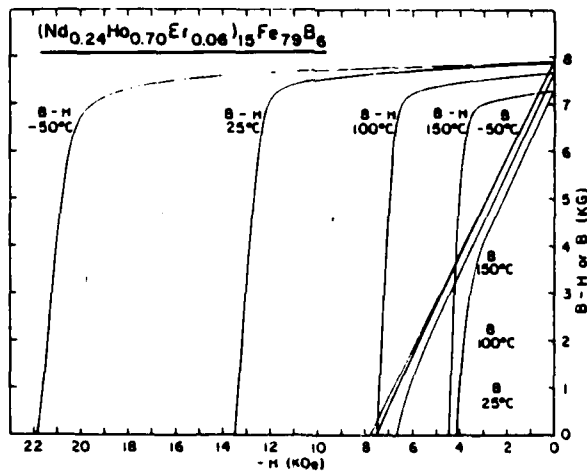


Figure 5. The temperature dependence demagnetization
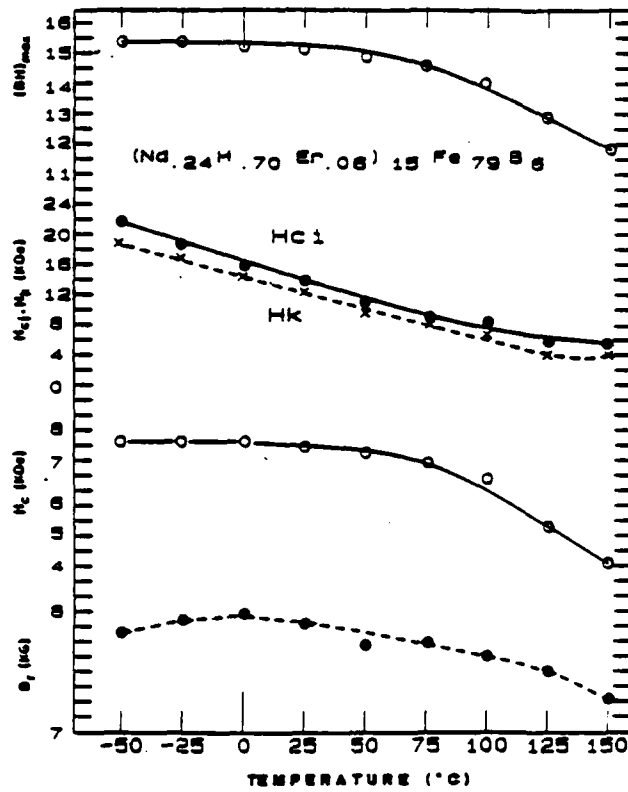curves of $(Nd_{0.24}Ho_{0.70}Er_{0.06})_{15}Fe_{79}B_6$.

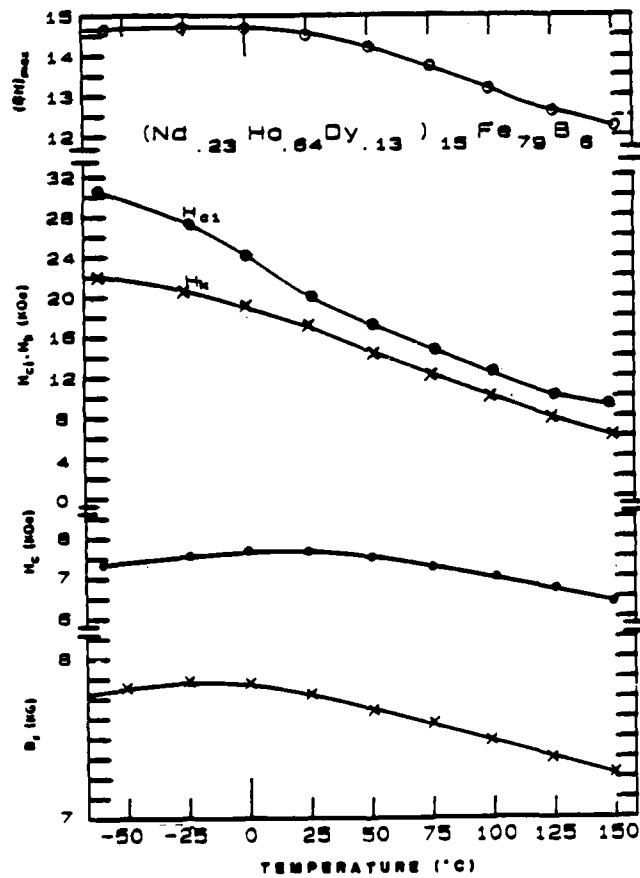Figure 6a. The temperature dependence magnetic
properties of Magnet A.



Figure 6b. The temperature dependence magnetic
properties of Magnet B.

Magnet A
$(Nd_{0.24}Ho_{0.70}Er_{0.06})_{15}Fe_{79}B_6$

Magnet B
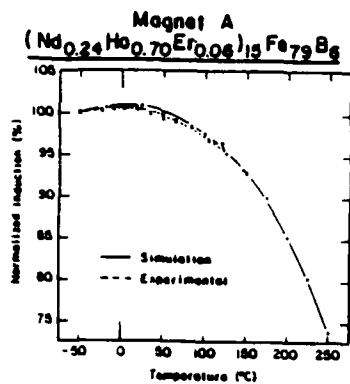$(Nd_{0.24}Ho_{0.64}Dy_{0.13})_{15}Fe_{79}B_6$

Figure 7                          Figure 8
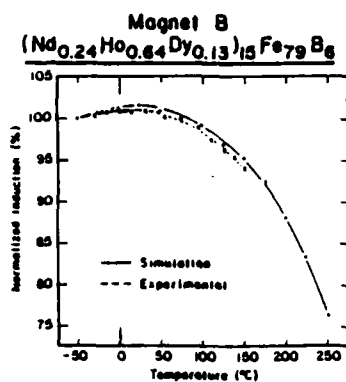
Figure 7. The experimental and computer simulated temperature dependence magnetization of Magnet A normalized to their values of -50°C.

Figure 8. The experimental and computer simulated temperature dependence magnetization of Magnet B normalized to their values of -50°C.

Table IV. The Comparison of the Temperature Coefficient α of the Experimental Results with Computer Simulated Results

| Magnet | % of R in $R_{15}Fe_{79}B_6$ | | | | | Temperature Coefficient [a] % per °C (-50 to +150) | |
|--------|----|----|----|----|----|----------------|------------|
|        | Nd | Ho | Dy | Er | Gd | experimental | simulation |
| A | 24 | 70 |   | 6 |   | -0.034 | -0.013 |
| B | 23 | 64 | 13 |   |   | -0.029 | -0.012 |
| C | 61 | 31 | 7 |   | 1 | -0.070 | -0.061 |
| D | 65 | 35 |   |   |   | -0.074 | -0.063 |

We have extended the computer technique for the computation of anisotropy field utilizing anisotropy field variation with temperature of $Nd_2Fe_{14}B$ and $(HRE)_2Fe_{14}B$ alloys. The room temperature anisotropy field compare within 5 kOe of the computed fields.

## CONCLUSION

Computer simulation technique employed produced alloy compositions that compare favorably with experimental observation on sintered magnets. Number of alloys with varying levels of temperature compensation are available from the rare earth-iron-boron alloys.

## ACKNOWLEDGEMENT

# REFERENCES

1. K. S. V. L. Narasimhan, J. Appl. Phys. 57, 4081, (1985).

2. M. Sagawa, S. Fujimura, N. Togawa, H. Yamamoto and Y. Matsuura, J. Appl. Phys. 55, 2083, (1984).

3. R. W. Lee, E. G. Brewer and N. A. Schaffel, IEEE Trans. Magn., MAG-21, 1958, (1985).

4. M. G. Benz, R. P. Lorfce and D. L. Martin, AIP Conf. Proc., No. 18, 1173, (1974).

5. K. S. V. L. Narasimhan, Proc. Fifth International Workshop on Rare Earth Cobalt Permanent Magnets and Their Applications, Roanoke, Va., June 1981, University of Dayton, p. 629 (1981).

6. H. A. Leupold, E. Potenziani, A. Tauber, and H. F. Mildrum, J. Appl. Phys. 55, 2097, (1984).

7. F. E. Camp and K. S. V. L. Narasimhan, IEEE Trans. Magn., MAG-21, 1970, (1985).

8. K. Sagawa, S. Fujimura, H. Yamamoto, Y. Matsuura, S. Hirosawa, and K. Hiraga, Proc. 8th International Workshop on Rare Earth Magnets and Applications, Ed. by K. J. Strnat, University of Dayton, p. 587 (1985).

FIGURES

1. Computer simulated temperature dependence magnetization curves of $(Nd_{1-x}Ho_x)_2Fe_{14}B$, where $x = 0$, .2, .4, .6, .8, and 1.0.

2. Computer simulated temperature dependence magnetization curves of $(NdHoEr)_2Fe_{14}B$, $(NdHoGd)_2Fe_{14}B$, and $(NdHoDyGd)_2Fe_{14}B$ on the corresponding sintered magnets with slightly higher Nd content.

3. Computer simulated temperature dependence magnetization curves of $(NdHoDy)_2Fe_{14}B$, $(NdHoDyGd)_2Fe_{14}B$ and $(NdHoEr)_2Fe_{14}B$ of the corresponding low temperature coefficient sintered magnets.

4. The temperature dependence demagnetization curves of $(Nd_{0.23}Ho_{0.70}Dy_{0.13})_{15}Fe_{79}B_6$.

5. The temperature dependence demagnetization curves of $(Nd_{0.24}Ho_{0.70}Er_{0.06})_{15}Fe_{79}B_6$.

6a. The temperature dependence magnetic properties of Magnet A.

6b. The temperature dependence magnetic properties of Magnet B.

7. The experimental and computer simulated temperature dependence magnetization of Magnet A normalized to their values of $-50^{\circ}C$.

8. The experimental and computer simulated temperature dependence magnetization of Magnet B normalized to their values of $-50^{\circ}C$.

END
DTIC
8-86